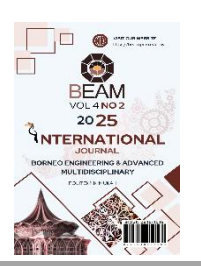


# Borneo Engineering & Advanced Multidisciplinary International Journal (BEAM)

Volume 4, Issue 2, November 2025, Pages 63-69



# Design and Development of an Electrical Power Prediction of a Small-Scale Hydrokinetic Turbine

Diana Ringgau<sup>1\*</sup>, Chen Wong Keong<sup>2</sup>, Bong Siaw Wee<sup>3</sup>

<sup>1</sup>Department of Electrical Engineering, Politeknik Mukah, KM 7.5 Jalan Oya, 96400, Mukah, Sarawak, Malaysia

<sup>2</sup>Department of Mechanical Engineering, Politeknik Kuching Sarawak, KM 22, Jalan Matang, 93050 Kuching, Sarawak, Malaysia

<sup>3</sup>Department of Electrical Engineering, Politeknik Kuching Sarawak, KM 22, Jalan Matang, 93050 Kuching, Sarawak, Malaysia

\*Corresponding author: dianaringgau@pmu.edu.my Please provide an official organisation email of the corresponding author

## **Full Paper**

Article history
Received
9 May 2025
Received in revised form
25 September 2025
Accepted
1 October 2025
Published online
1 November 2025



#### **Abstract**

Hydrokinetic turbine (HKT) technology harnesses kinetic energy from rivers with low slopes. Turbem software is frequently used to simulate and estimate the output power of HKT systems; however, its predictions often overestimate actual performance. To achieve more accurate estimates, a combination of Blade Element Momentum (BEM) theory and experimentation is recommended. In this study, a small-scale HKT system with a turbine diameter of 0.3 meters and a fixed blade angle of  $13^{\circ}$  was analyzed. BEM theory was employed to estimate the power coefficient (Cp) and the tangential-to-water flow velocity ratio ( $\lambda$ ), yielding a Cp value of 0.25 and a tip-speed ratio (TSR) of approximately 5. Based on these parameters, the optimal output power of a Direct Current (DC) Permanent Magnet Generator was determined to correspond to rotational speeds ranging from 196 to 343 rpm, considering a gear ratio of 1.75 and a transmission efficiency of 88%. The relationship between the generator's power output and its rotational speed was experimentally validated under full-load conditions, using 12 V DC LED bulbs as load resistors. The results demonstrated a strong correlation, with a R2 value of 0.9965. A predicted power output versus rotational speed graph was generated and compared with field data. The results revealed prediction errors of 16% for power output and 5% for rotational speed, which were deemed acceptable for river velocities between 0.8 and 1.4 m/s.

Keywords: - Small-scale hydrokinetic turbine, power prediction, driver

Copyright © This is an open access article distributed under the terms of the Creative Commons Attribution License



#### 1. Introduction

Hydrokinetics is a technology that extracts kinetic energy from river currents of almost zero elevation or lowland rivers. The amount of hydrokinetic energy contained in a stream depends on the river velocity (Yuce & Muratoglu, 2015). The technology utilizes a HKT system shown in Fig. 1, to convert the kinetic energy of the flowing river water into mechanical power. The generator then turns the mechanical strength into electrical power. Many remote village communities in Malaysia live near riverbanks for water supply, food, and transportation. For such cases, hydrokinetic energy is

considered by some researchers as a potential solution for off-grid rural community's electric power supply application (Tan et al., 2021).

It is important to estimate the power prediction that can be generated by the HKT system. Power prediction is imperative for determining the economic feasibility of technology. Predicting the power output allows for an assessment of whether the energy produced is adequate to meet the energy demands of the village communities. Accurate hydrokinetic turbine power prediction is critical for optimizing the design and performance of the turbine system. With precise power output estimates, different design options can be evaluated, and modifications can be

made to the turbine to enhance its performance. Furthermore, hydrokinetic turbine power prediction is significant for environmental impact assessment. Estimating the power output enables the assessment of the potential environmental impacts of a hydrokinetic turbine system, such as effects on aquatic life, water quality, and sediment transport. Accurate power predictions facilitate the identification of potential risks and ensure that appropriate measures are taken to minimize environmental impacts.

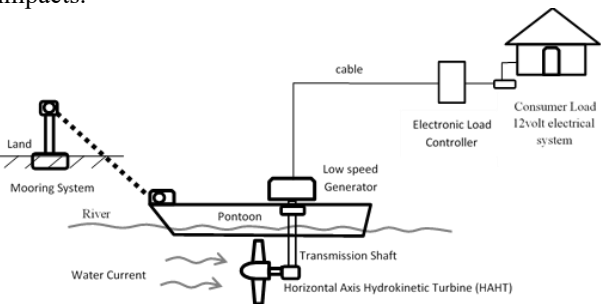


Fig. 1. The concept of hydrokinetic turbine system

Software design tools such as Turbem Computational Fluid Dynamics (CFD) are commonly used for the numerical simulation in the HKT system. However, the software's prediction is often less accurate as it typically overestimates the output power and operating point, which often exceeds experimental results. (Tian et al., 2018). The overestimation of the operating point occurs because mechanical friction and misalignment effects are not included in the BEM model used by the software (Muñoz et al., 2014), thus, it may require further validation through experiments. Another limitation of these software tools is the high computational requirements needed for these tools. They require powerful computers with high computational power, making them expensive and inaccessible to smaller research groups. In addition, the simulation process can be time-consuming, requiring significant time and effort to complete. The complexity of the software may also be a limitation, as it requires extensive knowledge and experience to operate and interpret the results, limiting its accessibility to nonexperts.

Field measurements, physical modeling and analytical modeling are several methods that can be used to produce power and output current predictions of hydrokinetic turbine energy. However, after carefully considering the advantages and limitations of each method, the most appropriate approach based on the specific project requirements and available resources is to propose the combination of Blade Element Momentum (BEM) theory and physical modeling to produce accurate predictions of power and output current for the system in a lowland river. The BEM theory is a commonly used method for predicting the performance curve of wind turbines, and it is also applicable to HKT system since they operate under the same principles as wind turbines (Patrick & Matthias, 2010). Therefore, the performance curve will be plotted at a fixed pitch angle to estimate the tip speed ratio and power

coefficient value of the HKT system. The tip speed ratio value will then be used to estimate the turbine rotational speed as a function of the river velocity's graph. Later, the physical modeling will complement the relationship between the generator's power output and the turbine rotation speed.

#### 1.1 Blade Element Momentum Theory

The efficiency of a hydrokinetic turbine's rotor in converting the kinetic energy of water flow into mechanical energy directly impacts its electrical power output. This efficiency is primarily influenced by the generator's electrical load and the rotor's TSR (Puertas-Frias et al., 2022 & Lust et al., 2018).

Optimal hydrodynamic performance is achieved when the TSR is at its ideal value, meaning the rotor blades are moving at a speed that maximizes energy extraction from the water flow. Tip speed ratio or TSR,  $\lambda$  for turbine is the ratio between the tangential speed of the tip of a blade and the actual speed of the water current, v. The TSR is related to efficiency, with optimum efficiency varying with blade design. Identifying the right TSR for the designed turbine that matches the river velocities is crucial. The definition of  $\lambda$  is

$$\lambda = \frac{R\omega}{v} = \frac{R}{v} \left(\frac{2\pi}{60}\right) N \tag{1}$$

where  $\omega$  is angular rotation in rad/s, N is rotation speed in m/s, R is the radius of the designed turbine and v is the velocity of a river. The performance curve is always associated with the turbine output power. The turbine output power definition is in equation (2) where  $\rho$  is a function of fluid density, with A is the swept area of the turbine, v is the velocity of river,  $C_p$  is the power coefficient and  $\eta$  is the drive train efficiency such as efficiency generator and gear ratio.

The relationship between  $P_m$ ,  $C_p$ , and v are shown in equations (2) and (3).  $P_m = \frac{1}{2} \rho A v^3 \times C_P \times \eta$ 

$$P_m = \frac{1}{2}\rho A v^3 \times C_P \times \eta \tag{2}$$

According to Betz's theoretical limit, Cp is less than 0.593, and Cp is given as

$$C_P(\lambda, \theta) = 0.22(\frac{116}{\lambda_i} - 0.4\theta - 5)e^{-\frac{12.5}{\lambda_i}}$$
 where,  

$$\frac{1}{\lambda} = \frac{1}{\lambda + 0.08\theta} - \frac{0.035}{\theta^3 + 1}$$
 (3)

The angle between rotor plane and blade tip chord is known as the pitch angle,  $\theta$ . The angle and the TSR were used in equations (2) and (3) to characterize the turbine power performance as well as monitor the turbine behavior over time. According to Donald (2017), the maximum Cp of the turbine does not correspond to the maximum power output of the generator, Pg. However, the study of Cp was made to identify the range and relationship of v and

rotational speed of the turbine rotor, Nt, that corresponded to each Pm production. The electrical load influences the rotor's rotational speed (N), which in turn affects the tip speed ratio (TSR,  $\lambda$ ). A high electrical load increases mechanical torque, slowing the rotor and reducing TSR, potentially leading to suboptimal Cp. Conversely, a low electrical load allows the rotor to spin faster, possibly exceeding the optimal TSR and reducing Cp, which lowers power capture. Therefore, the maximum Cp does not necessarily correspond to the maximum generator output power (Pg). This indicates that generator efficiency, losses, and electrical load dynamics also play a crucial role in determining actual electrical power output. The angle between rotor plane and blade tip chord is known as the pitch angle,  $\theta$ . The angle and the TSR were used in equations (2) and (3) to characterize the turbine power performance as well as monitor the turbine behavior over time. According to Donald (2017), the maximum Cp of the turbine does not correspond to the maximum power output of the generator, Pg. However, the study of Cp was made to identify the range and relationship of v and rotational speed of the turbine rotor, Nt, that corresponded to each Pm production. The electrical load influences the rotor's rotational speed (N), which in turn affects the tip speed ratio (TSR,  $\lambda$ ). A high electrical load increases mechanical torque, slowing the rotor and reducing TSR, potentially leading to suboptimal Cp. Conversely, a low electrical load allows the rotor to spin faster, possibly exceeding the optimal TSR and reducing Cp, which lowers power capture. Therefore, the maximum Cp does not necessarily correspond to the maximum generator Pg. This indicates that generator efficiency, losses, and electrical load dynamics also play a crucial role in determining actual electrical power output.

#### 2. Methodology

A physical model of the rotor was constructed with a 0.3 m diameter and a fixed pitch angle to experimentally analyze its performance. equation (3) was applied to estimate the tip  $\lambda$  and Cp when the pitch angle was set to  $13^{\circ}$ , resulting in a Cp value of 0.25 for a TSR of approximately 5. These values were then used to determine the turbine Nt and the corresponding river velocity. The relationship between Nt and the river velocity was derived as in equation (4).

$$N_T = \frac{350}{11} \lambda \nu \tag{4}$$

Equation (4) represents the relationship applied in this study for estimating Nt under varying river velocities. Furthermore, equation (2) and the graph of  $Cp(\lambda, 13^{\circ})$  from Fig. 2 were used to plot the Pm-Nt characteristics. The swept area (A) was calculated as  $\pi R^2 = 0.28$  m², and the water density ( $\rho$ ) was assumed to be  $1000 \text{ kg/m}^3$ . The swept area is determined by the rotor's mechanical dimensions, while water density depends on environmental factors such as temperature and salinity. The river velocity was considered a variable parameter, influenced by seasonal

changes in rainforest environments. From Fig. 2, at the optimum operating condition where Cp = 0.25, the river v was 1.4 m/s, leading to a Nt of 222.7 rpm and an estimated mechanical Pm of 84.6 W. At a lower river velocity of 0.8 m/s, Nt decreased to 127 rpm, and the estimated Pm was 15.8 W. However, since numerical estimations often overpredict experimental power, the Pm-Nt characteristics derived here serve only as a reference and are not expected to be numerically exact. The data extracted from Fig. 2 was used to determine an appropriate transmission gear ratio and generator rated power, ensuring the hydrokinetic turbine (HKT) operates at maximum efficiency, as guided by the approach of Kusakana (2018).

Fig. 2. Illustrates the characteristic curve of Pm-Nt for the designed rotor, which was used in this study to estimate turbine performance under varying river velocities. This graph was generated using equation (2) and the  $Cp(\lambda,13^\circ)$  relationship, serving as a reference for selecting an optimal transmission gear ratio and generator rated power to maximize HKT performance. These values were considered during the system design phase before conducting physical experiments.

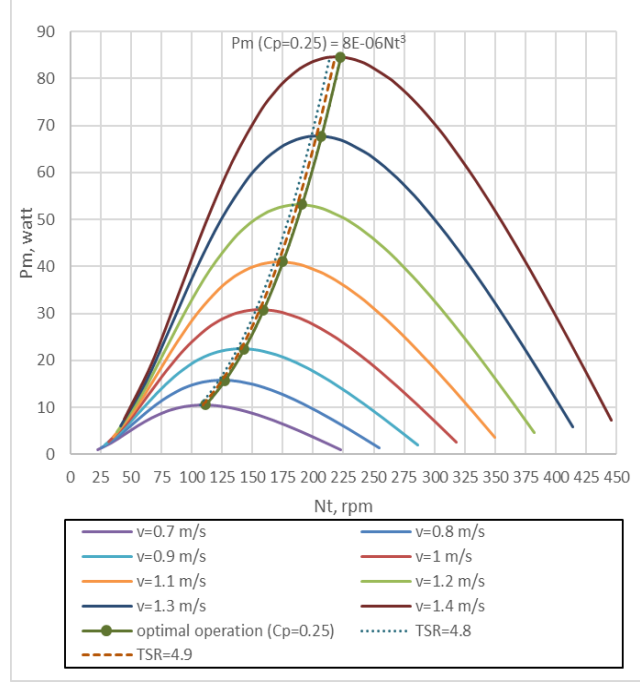


Fig. 2: The characteristic curve of *Pm-Nt* for the designed rotor

The Nt amplified the rotational speed of the generator (Ng) by using a 90° transmission gear with 1:1.75 ratio. For maintaining standard safety, Ng could not exceed the rated speed of HKT's generator by more than 80%. However, for higher efficiency of the generator, Ng should always be within the generator rated speed. Therefore, based on equations (1) and (4) with a gear ratio of 1.75 and  $\eta$  is the transmission part efficiency, which is 88%, then Ng can be determined as in equation (5).

$$N_g = 245v \tag{5}$$

Therefore, the generator rotational speed was expected to be between 196 rpm to 343 rpm. However, the minimum value of Ng and v can only be determined from the prediction graph of the electrical power production. This is because the HKT system is only used to export energy when the river has reached enough velocity to transfer its kinetic energy into the turbine rotor or in other words, when the turbine has exceeded its cut-in speed.

#### 2.1 Experiment Setup and Procedure

In addition to theoretical modeling using Blade Element Momentum (BEM) theory, a physical model was developed to enhance the accuracy of power and output current predictions for the HKT system in a lowland river environment. This section describes the experimental setup and procedures undertaken to validate the generator's performance under both no-load and load conditions.

The Permanent Magnet DC (PMDC) motor, model My1018 was used as a generator for the HKT system. The motor produced 24 V at a rated speed of 420 rpm. It can operate at low rotational speeds and provide outstanding efficiency, especially in low flowing river conditions, as its cut-in point is relatively small. The no-load test was conducted to evaluate the generator's output voltage and current at various rotational speeds when no external load was connected. This test allowed for the assessment of the generator's internal losses and the establishment of its operating characteristics in the absence of a load. By measuring the generator's performance under no-load conditions, valuable insights were gained into its efficiency and internal behavior.

Conversely, a load test was performed to examine the generator's performance under different load conditions, which could vary in a hydrokinetic turbine system due to changing water flow. Its procedure can be summarized in the flowchart shown in Fig. 3. It was crucial to understand how the generator responded to these load variations. During the load test, a load resistance, consisting of nine pieces of 12 V DC LED bulbs, was connected in parallel arrangement with each bulb having a switch in series shown in Fig. 4. Activating a switch created a resistance of  $16~\Omega$ , connecting the load resistance to the generator's output terminal.

To ensure compliance with the 12 V electrical system and consider the characteristics of the designed rotor in relation to the river velocity as described in equation (5), the load test was conducted by driving the generator with a prime mover at speeds ranging from 196 rpm to 343 rpm. The rotational speed of the generator's shaft was carefully adjusted to maintain a constant voltage output of 12 V.

The generator was operated at its rated speed for a duration of half an hour, which allowed for the stabilization of temperatures in the generator's rotor and magnets, ensuring consistent and reliable measurements. Therefore, after this period, nine measurements of Pg, current, and voltage were recorded and repeated three times to ensure consistency.

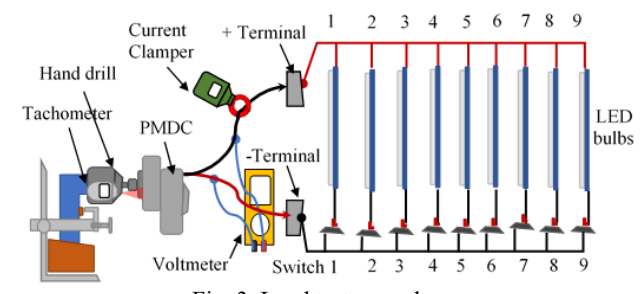


Fig. 3. Load test procedure

By identifying the rotation speed that yields the highest output power and current, the optimal operating conditions for the generator can be determined. The relationship helps with the design and sizing of the hydrokinetic system. It provides insights into the required rotation speed of the generator to achieve the desired power output and current levels. Moreover, this relationship can be utilized in predictive modeling. It enables the estimation of power generation capabilities under different operating conditions and facilitating energy production forecasting.



Fig. 4. Load-condition setup with the 12 V system

#### 2.2 Field Measurements

The HKT system was fabricated and deployed at Sungai Sarawak Kiri, Sarawak. Fig. 5 shows the field site measurement setup. The experiment was observed under flow conditions of 1.2 m/s, while the suitable gearing ratio was selected to match the rotation rate of the designed turbine blade. Table 1 provides additional details regarding the HKT system specification. The HKT system was intended to align with the concept shown in Fig. 1; however, due to a technical problem, the Electronic Load Controller (ELC) was excluded from this setup. As a result, the electrical power output of the HKT system was not stabilized, and it was unable to actively regulate the load to maintain a stable output voltage and frequency.

Consequently, the system did not compensate for fluctuations in the water flow or turbine speed, and it was unable to adjust and adapt to changes in these variables, resulting in an unstable power output.

Real-time operation data was recorded using a data logger, which collected data from various sensors and measurements within the HKT system. This data includes v, Ng, generator output voltage, and Iout. Data preprocessing was performed to handle missing values, outliers, and noise in the collected data. Additionally, to

address the impact of fluctuations in the turbine speed on the Cp and TSR of the HKT system, data normalization was applied to ensure that all features are on a similar scale.

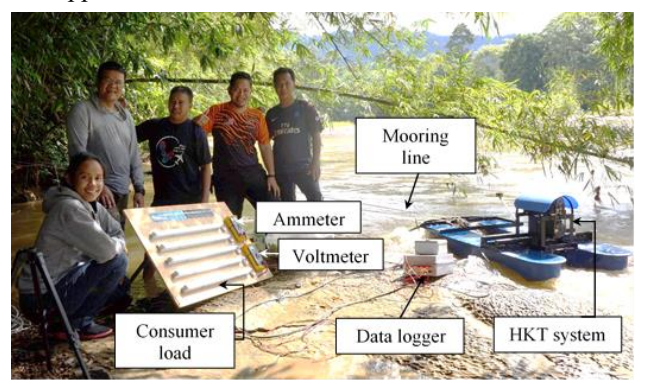


Fig. 5. The field site measurement setup

Table 1: The HKT system specification

	Physical model	
1	Diameter of rotor	0.3 m
2	Rotor's fixed pitch angle	13°
3	$C_p$	0.25
4	TSR (λ)	5
5	Transmission gear ratio	1:1.75
6	η	88%

Field site measurements were carefully selected and filtered based on specific TSR values (4.8, 4.9, 5.0, and 5.1). These values were selected to establish new relationships between v and Ng, utilizing the same technique used to derive equation (5). Subsequently, these relationships were utilized to validate the predicted graph. To determine the performance of the proposed methods, the measurement from field site was filtered and compared with the predicted value. The only way to assess the accuracy of the predicted value is to compare this value with known true or actual value. Usually, Root Mean Square error (RMSE) and Mean Absolute Error (MAE) are used to identify HAHT power forecasting performance. The RMSE or is given by:

$$e_{RMSE} = \frac{\sqrt{\sum_{t=1}^{N} (P_t^{act} - P_t^{pred})^2}}{P_{cap}\sqrt{N}}$$

$$e_{MAE} = \frac{\sum_{t=1}^{N} |P_t^{act} - P_t^{pred}|}{P_{cap} \times N}$$
(6)

$$e_{MAE} = \frac{\sum_{t=1}^{N} |P_{t}^{act} - P_{t}^{pred}|}{P_{cap} \times N}$$
 (7)

where  $P_t^{act}$  is the actual measured value of the output power of a single unit HAHT at time, t. Ppred is the predicted value of output power (Watt) of a HAHT or single unit at t;  $P_{cap}$ is the HAHT installed capacity; and N is the total number of samples.

### 3. Result and Discussion

Fig. 6 presents the experimental results, illustrating the relationship between the v, *Iout*, and *Pg* with respect to the rotational speed of the generator. The results indicate direct proportionality among these variables, where an increase in generator speed leads to a corresponding rise in output power and current. The plotted linear trendlines for Pg and *Iout* as functions of generator speed exhibit  $R^2$  values of 0.9965 and 0.9966, respectively, demonstrating a strong correlation. This high degree of linearity confirms that generator speed plays a significant role in determining both power and current output. The consistency of these results suggests that the system operates with predictable performance under varying load conditions.

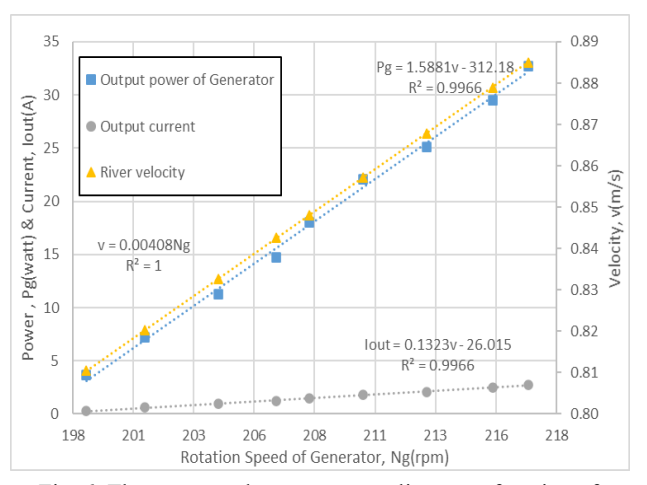


Fig. 6. The power and output current lines as a function of rotational speed of generator at  $\eta$ =88%

Fig. 7 was extrapolated based on the results shown in Fig. 6, extending the analysis up to the generator's rotational speed limit of 378 rpm. Fig. 7 shows that the turbine began exporting energy when the river velocity reached 0.78 m/s, surpassing its cut-in speed at around 190 rpm. Turbine speed fluctuations, which directly affect the rotor blade tip speed, can change the value of  $\lambda$ . Higher turbine speeds result in increased  $\lambda$ , indicating more energy extraction from the water flow. However, if the  $\lambda$  value exceeds 5.1, this indicates Nt would rotate too fast, and Ng would spin at over 390 rpm. Consequently, the HKT system would only rotate through turbulent water and not effectively harness the power. In other words, even if Ng would rotate faster than 390 rpm, the system would not produce more power. Therefore, the prediction graph is limited to Cp at 0.25, rotor's radius at 0.3 m,  $\theta$  at 13°, and a 12 V electrical load for the system. The maximum Cp value of 0.25 is achieved when  $\lambda$  is around 4.8 to 5.1, as shown in Fig. 2.

Fig. 8, 9 and 10 were plotted to verify the reliability of the predictive graph in Fig. 7. The selected field site data was then compared by matching their  $\lambda$  value to the  $\lambda$  value of the predicted graph. Then, from the treated data, the predicted values of Pg were determined by their nearest value with the field site's. The nearest predicted Vt values were also determined in a similar manner to the predicted Pg values, and this was followed by the prediction of *lout* values, which were identified based on the predicted Vt values.

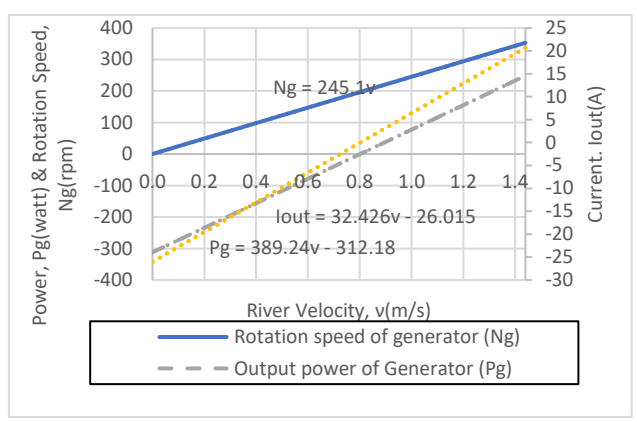


Fig. 7. Prediction graph of electrical power production at  $\lambda$ =5,  $\eta$ =88%

Equation (7) was used to determine the MAE of the prediction graph because it is a suitable method for quantifying the discrepancy between predicted and observed values. The accuracy of river velocity measurements is a critical factor in HAHT performance evaluation. However, due to the requirement that the velocity sensor be positioned very close to the rotor, slight variations in placement may introduce measurement inaccuracies. These inaccuracies can affect the predicted power output, as HAHT power curves ideally correlate with river velocity.

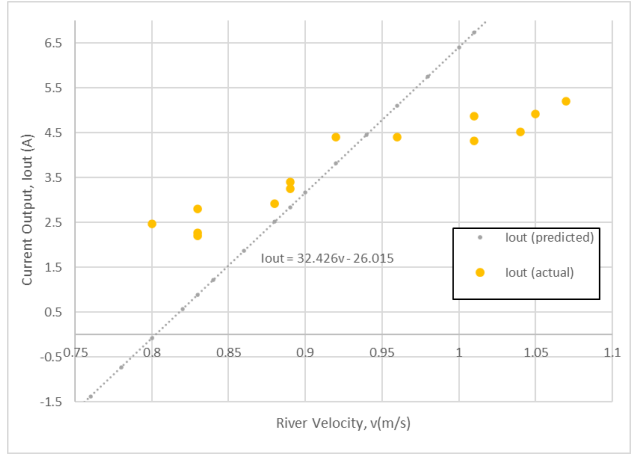


Fig. 8. The comparison of output current (Iout) produced by generator between the predicted and field site measurement

The MAE calculation provides a direct measure of how closely the prediction graph aligns with actual experimental data. A lower MAE value indicates a higher degree of accuracy, ensuring that the model effectively represents real-world conditions. The prediction data for *Iout*, *Pg*, and *Ng* exhibited MAE values of 21%, 16%, and 5%, respectively. Among these, *Iout* experienced the highest error, suggesting that improvements in data

collection, such as increasing the number of samples could enhance prediction accuracy.

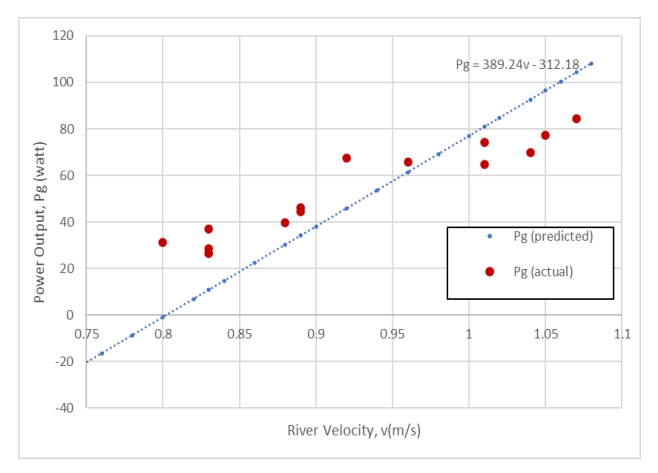


Fig. 9. The comparison of output current (*lout*) produced by generator between the predicted and field site measurement

A larger experimental dataset would enable a more precise estimation of the power curve across a broader range of river velocities and generator speeds. This, in turn, would refine the model's predictive capability, reduce uncertainty and improve alignment with actual system performance.

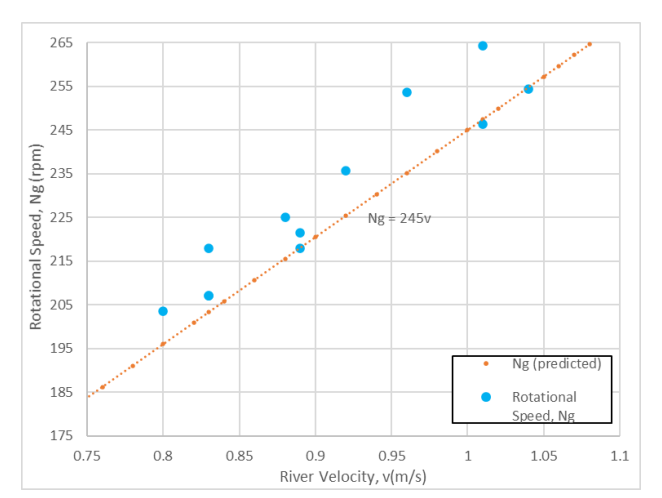


Fig. 10. The comparison of generator's rotation speed, Ng between the predicted and field site measurement

The accuracy of the predicting data could be further improved by refining the prediction model itself through the incorporation of nonlinear regression techniques or machine learning algorithms. Moreover, conducting validation experiments under varied water depths, and temperature variations will ensure the robustness of the model across different environmental scenarios. Synchronizing sensor data collection with generator measurements is also essential to eliminate time-laginduced errors.

#### 4. Conclusion

In conclusion, this research aimed to develop a predictive model for HKT energy specifically designed for 12-volt electrical system applications in lowland rivers or channels with low flow rates. The performance of the prediction graph was assessed by comparing it with measurement data from the field site. The results showed a reasonable level of consistency between the predicted trends and the actual measurement values within the river velocity range of 0.8 - 1.4 m/s. Although the prediction data for Pg and Ng exhibited Absolute Error percentages of 16% and 5% respectively, they were considered acceptable given the functional specification requirements for wind power forecasting systems. Furthermore, the prediction graph for Ng demonstrated a close approximation to the actual data, indicating a higher level of accuracy. This research provides valuable insights for site model calibration and validation, enabling the optimization of hydrokinetic energy systems. It also serves as a foundation for future model development and offers input data for further analysis and refinement. Moving forward, the predictive power of HKT energy can be leveraged to estimate the cost-effectiveness of the system's energy production. Overall, this study contributes to the advancement of hydrokinetic energy technology and opens avenues for its practical implementation in lowland river environments.

**Author Contributions:** The research study was carried out successfully with contributions from all authors.

Conflicts of Interest: The authors declare no conflict of interest.

#### References

- Donald, M. R. (2017). Instrumentation platform and Maximum Power Point Tracking control for a Hydrokinetic turbine. Universidade de Brasília.
- Kusakana, K. (2018). Optimization of the daily operation of a hydrokinetic diesel hybrid system with pumped hydro storage Optimization of the daily operation of a hydrokinetic diesel hybrid system with pumped hydro storage. *Energy Conversion and Management*, 106(December 2015), 901–910.
  - https://doi.org/10.1016/j.enconman.2015.10.021.
- Lust, E. E., Flack, K. A., & Luznik, L. (2018). Survey of the near wake of an axial-flow hydrokinetic turbine in quiescent conditions. *Renewable Energy*, 92-101.
- Muñoz, A. H., Chiang, L. E., & Jara, E. A. De. (2014). A design tool and fabrication guidelines for small low cost horizontal axis hydrokinetic turbines. *Energy for Sustainable Development*.
  - https://doi.org/10.1016/j.esd.2014.05.003.
- Patrick, M, Matthias, W, S. B. & J. P. (2010). Power curves for wind turbines. In *Power curves for wind turbines* (Vol. 44, pp. 565–611). Oldenburg, Germany: WIT Transactions on State of the Art in Science and Engineering.
  - https://doi.org/10.2495/978-1-84564.
- Puertas-Frías, C. M., Willson, C. S., & García-Salaberri, P. A. (2022). Design and economic analysis of a hydrokinetic turbine for household appliance. Renewable Energy Journal, 587–598.
- Tan, K. W., Kirke, B., & Anyi, M. (2021). Small-scale hydrokinetic turbines for remote community electrification. *Energy for Sustainable Development*, 63, 41-50.
- Tian, W., Mao, Z., & Ding, H. (2018). Design, test and numerical simulation of a low-speed horizontal axis hydrokinetic turbine. *International Journal of Naval Architecture and Ocean Engineering*, *10*(6), 782–793. https://doi.org/10.1016/j.ijnaoe.2017.10.006.
- Yuce, M. I., & Muratoglu, A. (2015). Hydrokinetic energy conversion systems: A technology status review. Renewable and sustainable energy reviews, 43, 72-82.